doi.org/10.36721/PJPS.2026.39.10.280.1

Integrative *in-silico*, *in-vitro and in-vivo* assessment of [W_4KR_5]-curcumin conjugates as potential anti-inflammatory and antinociceptive therapeutics

Syeda Nazish Sohaib[1], Syed Muzzammil Masaud[1]*, Yasir Rasool[1], Mohammad Imran Sajid[2], Sana Ayaz[1], Abida Shamim[1] and Sohaib Zafar Malik[1]*

[1]Riphah Institute of Pharmaceutical Sciences, Riphah International University, Islamabad, 44000, Pakistan
[2]Faculty of Pharmaceutical Science, University of Central Punjab, Lahore, 54000, Pakistan

Abstract: **Background**: Curcumin is well recognized as a natural anti-inflammatory and analgesic compound; however, its application in clinical conditions is hindered by its poor bioavailability and moderate potency. Peptide conjugation modification is a promising approach to enhance its potency. **Objectives**: The purpose of this study was to design, synthesize and evaluate new cyclopeptide-curcumin conjugates to enhance cyclooxygenase inhibition, anti-inflammatory efficacy and antinociceptive effects. **Methods**: Three cyclopeptide–curcumin conjugates—[W_4KR_5]-5-oxopentanoate-curcumin, [W_4KR_5]-3,5-dioxopentanoate-curcumin and [W_4KR_5]-12-oxododecanoate-curcumin—were investigated using integrated *in-silico*, *in-vitro and in-vivo* approaches. Molecular docking was performed against COX-1 (PDB ID: 3N8X) and COX-2 (PDB ID: 1PXX). *In-vitro COX inhibition assays assessed enzyme selectivity. At the same time, in-vivo antinociceptive and anti-inflammatory activities were evaluated using acetic acid–induced writhing, tail immersion, formalin-induced pain and* carrageenan-induced paw edema. **Results**: All conjugates demonstrated superior binding affinity to COX enzymes compared to curcumin, with [W_4KR_5]-12-oxododecanoate-curcumin exhibiting the strongest COX-2 interaction (−11.4 kcal/mol vs. −7.8 kcal/mol for curcumin), stabilized by key residues Tyr385, Ser530 and Arg120. This compound showed marked COX-2 selectivity *in-vitro* (IC_{50} = 0.82 μM) relative to COX-1 (IC_{50} = 4.65 μM), outperforming curcumin (COX-2 IC_{50} = 6.21 μM). *In-vivo*, it significantly reduced acetic acid–induced writhing (72.4%), increased tail immersion latency (63.1%), suppressed formalin-induced neurogenic (61.7%) and inflammatory (75.5%) pain phases and inhibited carrageenan-induced paw edema by 68.2%, compared to 39.4% for curcumin. **Conclusion**: The conjugation of cyclopeptide significantly increases the anti-inflammatory and antinociceptive potency of curcumin. Of the tested analogs, [W_4KR_5]-12-oxododecanoate-curcumin is particularly noteworthy as a lead compound worthy of further studies.

Keywords: Antinociceptive activity; Anti-inflammatory agents; Curcumin derivatives; Cyclopeptides; COX-2 inhibitors; Peptide–protein docking

Submitted on 13-12-2025 – Revised on 24-02-2026 – Accepted on 08-03-2026

INTRODUCTION

Pain and inflammation are the top stumbling blocks in medicine. Chronic pain syndromes, such as neuropathic and inflammatory pain, represent 20% of the global population. Inflammatory diseases, such as arthritis, inflammatory bowel disease and neuroinflammation, remain obstacles despite the use of nonsteroidal anti-inflammatory drugs (NSAIDs), corticosteroids and biologic therapies (Hunter and Bierma-Zeinstra, 2019). The current pharmacotherapies for these diseases face problems such as side effects, drug resistance and low effectiveness, making it necessary to develop new drugs with greater safety and efficacy.

Natural products have historically provided a valuable template for the development of active therapies for inflammation and pain. In this context, curcumin, a polyphenolic compound derived from Curcuma longa, has attracted significant attention due to its pleiotropic pharmacological activities, including anti-inflammatory, antinociceptive, antioxidant and anticancer effects (Gupta *et al*., 2012). The pharmacological effects of curcumin involve multiple molecular targets, such as cyclooxygenase-2 (COX-2), lipoxygenase, nuclear factor kappa B (NF-κB), inducible nitric oxide synthase (iNOS) and several cytokines (Aggarwal and Sung 2009; Hewlings and Kalman.

As a potential clinical drug, the application of curcumin is severely limited by its low water solubility, rapid oral metabolism and short half-life of absorption/bioavailability (Anand *et al*., 2007). This led to low plasma levels of the drug, which, in turn, limited the pharmacokinetics of curcumin as a typical drug. To overcome these constraints, scientists have explored structural modifications of CUR, nanocrystal formulations and prodrug formulations to enhance the bioavailability and solubility of curcumin

**Corresponding author:* e-mail: sohaibzafarmalik@gmail.com ; dr.muzamil15@gmail.com

(Anand *et al*., 2007, Nelson *et al*., 2017, Tabanelli *et al*., 2021). Among the most targeted treatments, Peptide conjugation was a strategy to increase curcumin delivery and bioactivity (Kaur *et al*., 2024).

Antimicrobial peptides (AMPs) play a role in host defense. They are cationic, amphipathic compounds that modulate the immune system (Mahlapuu *et al*., 2016), apart from AMPs, which also have immunomodulatory, wound-healing, antimicrobial and anti-inflammatory effects through cytokine induction suppression, modulation of Toll-like receptors (TLRs) and downregulation of oxidative stress [(Haney and Hancock, 2013)]. In this regard, synthetic analogs of AMPs have been designed to enhance these functions and minimize cytotoxicity (Mahlapuu *et al*., 2020, Kumar *et al*., 2018). In this context, our laboratory has previously described the design and synthesis of [W_4KR_5]-curcumin conjugates employing three different linkers, which showed strong antibacterial and membrane-disrupting activity against multidrug-resistant bacteria (Mohammed *et al*., 2022). This amphipathic peptide was designed to enhance electrostatic binding to negatively charged microbial membranes (Kumar *et al*., 2018, Wimley, 2010), with its hydrophobic tryptophan moieties promoting membrane insertion and destabilization.(Chan *et al*., 2006).

Since [W_4KR_5] is amphipathic and facilitates the solubilization of hydrophobic molecules (Mahlapuu *et al*., 2016), we hypothesized that conjugating curcumin to [W_4KR_5] might enhance curcumin's pharmacokinetics and its pain-relieving and anti-inflammatory properties. The bioconjugate combines the advantages of a peptide and a small molecule: the peptide for solubilization and targeting and curcumin for its anti-inflammatory properties (Albada and Metzler-Nolte, 2016, Mahlapuu *et al*., 2016).

Mechanistically, curcumin inhibits prostaglandin synthesis via the inhibition of COX and LOX pathways, as well as the inhibition of NF-κB-mediated inflammatory cytokine synthesis, including TNF-α, IL-1β and IL-6 (Jurenka, 2009). On the other hand, positively charged peptides such as [W_4KR_5] can modulate immune activation by neutralizing bacterial endotoxins. (Mookherjee and Hancock, 2007). These two components combine to make a rational designed treatment for inflammatory pain.

Even before conducting in silico experiments, molecular docking is used to assess these conjugates; computer simulations can predict how well the molecules will bind to the major inflammatory targets, the COX-2, iNOS and TRPV1 receptors. Computer simulations of ADME properties provide initial insights into oral absorption, blood-brain barrier penetration and metabolic stability (Daina *et al*., 2017). By integrating simulations with laboratory enzyme inhibition assays and animal experiments, we can assess [W_4KR_5]-curcumin derivatives. In the current study, the [W_4KR_5]-curcumin conjugates were subjected to *in silico docking studies to target COX-2, followed by in-vitro studies to assess their antioxidant and anti*-inflammatory properties. Finally, the *in-vivo* studies were conducted using the carrageenan-induced paw edema model and the formalin-induced nociception model. These models have been widely used to assess the anti-inflammatory and antinociceptive properties of compounds in preclinical studies (Winter *et al*., 1962).

The primary hypothesis is that conjugation of curcumin with [W_4KR_5] will provide greater pharmacological efficacy than free curcumin, due to increased solubility, stability and synergistic effects. The findings of this study are expected to provide important insights into the development of multifunctional peptide-polyphenol conjugates as the next generation of therapeutic agents for inflammatory pain.

MATERIALS AND METHODS

The synthesis and detailed physicochemical characterization of the [W_4KR_5]–curcumin conjugates have been previously reported by our group (Sohaib *et al*., 2025). Chemical structures of conjugates used in present study are shown in Fig. 1. Briefly, the conjugates were prepared using established solution-phase peptide conjugation strategies and purified by preparative reverse-phase chromatography to achieve high analytical purity. Structural confirmation and purity assessment were validated through NMR, FTIR, ESI-MS, CHN analysis and analytical HPLC, with all compounds exhibiting ≥95% purity. In the present study, these previously validated conjugates were directly employed for an integrative in silico, *in-vitro* and *in-vivo* evaluation of their anti-inflammatory and antinociceptive potential.

In-silico molecular docking

Methodology

Protein preparation

Crystal structures of COX-1 (PDB ID: 3N8X) and COX-2 (PDB ID: 1PXX) were retrieved from the Protein Data Bank (Kurumbail *et al*., 1996, Vecchio *et al*., 2010).The selected crystal structures represent conserved mammalian isoforms of Cyclooxygenase-1 and Cyclooxygenase-2, with preserved catalytic-site architecture. Docking was performed within the co-crystallized ligand-binding site and protocol validation by re-docking the native ligand yielded an RMSD < 2.0 Å, confirming methodological reliability. Water molecules, non-essential ions and heteroatoms were removed, while hydrogen atoms were added to optimize protonation states at physiological pH using UCSF Chimera 1.15 (Pettersen *et al*., 2004). The structures were minimized with the AMBER ff14SB force field to relieve steric clashes.

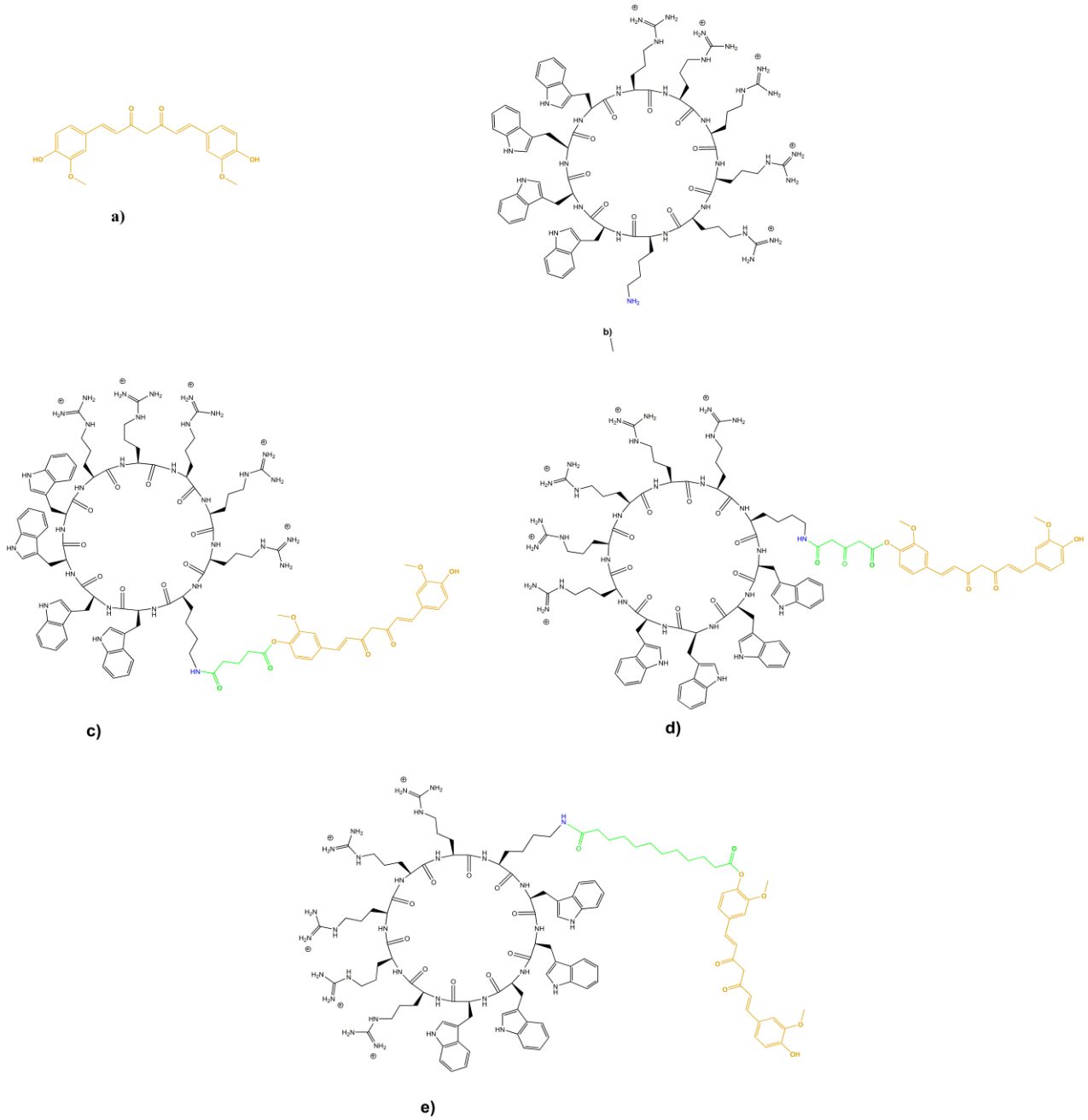

Fig. 1: Structure of Curcumin and cyclopeptide derivatives of Curcumin. (a) Curcumin; (b) W_4KR_5; (c) [W_4KR_5]-5-Oxopentanoate-Curcumin; (d) [W_4KR_5]-3,5-Dioxopentanoate-Curcumin; (e) [W_4KR_5]-12-Oxo-dodecanoate-Curcumin.

Peptide modeling

Three cyclic peptide derivatives of curcumin were modeled:
[W_4KR_5]-5-oxopentanoate-curcumin
[W_4KR_5]-3,5-dioxopentanoate-curcumin
[W_4KR_5]-12-oxododecanoate-curcumin
Initial structures were built in Avogadro 1.2 and refined using GROMACS 2022. Peptide cyclization was confirmed by energy minimization under the CHARMM36 force field (Huang and MacKerell Jr, 2013).

Peptide–protein docking

Peptide–Protein docking was carried out using the HADDOCK 2.4 webserver (Van Zundert *et al*., 2016). Active residues were defined around the COX catalytic domains (Arg120, Tyr355, Ser530 for COX-1; Val349, Tyr385, Ser530 for COX-2) (Picot *et al*., 1994). Cyclic peptides were uploaded as binding partners and docking was performed with standard parameters. The top 200 solutions were clustered using RMSD cutoffs of 2.0 Å and the best cluster was selected based on HADDOCK scores, van der Waals, electrostatic and desolvation energies.

For validation, peptide–protein docking was also performed with ClusPro-PP (Kozakov *et al*., 2017) and Rosetta FlexPepDock (Raveh *et al*., 2010). Binding free energies (ΔG, kcal/mol) and predicted dissociation constants (Kd, μM–nM range) were estimated using PRODIGY (Xue *et al*., 2016).

Active residues were defined based on structurally conserved catalytic and inhibitor-binding regions of Cyclooxygenase-1 and Cyclooxygenase-2, supported by co-crystallized ligand interactions. HADDOCK 2.4 was employed using standard data-driven parameters to incorporate biologically relevant restraints. Peptide flexibility was treated through semi-flexible refinement in HADDOCK, rigid-body docking in ClusPro-PP and high-resolution backbone refinement in Rosetta FlexPepDock, ensuring complementary sampling strategies and robust validation.

In-vitro cyclooxygenase (COX) inhibition assay

The inhibitory activity of synthesized compounds against COX-1 and COX-2 was evaluated using a commercially available enzyme immunoassay kit (Cayman Chemical, USA), following the manufacturer's protocol. The assay is based on competitive binding between prostaglandin (PG) generated by COX enzymes and a PG–acetylcholinesterase conjugate, using a limited number of PG-specific antibodies. (Chemical, 2024).

Recombinant COX-1 and COX-2 enzymes were incubated with test compounds at varying concentrations (1–100 μM) in reaction buffer containing arachidonic acid as the substrate at 37 °C. Each concentration was tested in triplicate (n = 3) within a single experiment and the entire assay was independently repeated three times to ensure reproducibility. Comparable experimental designs have been reported in recent studies evaluating COX inhibitory activity *in-vitro* using Cayman Chemical kits (Rudrapal *et al*., 2023). The enzymatic reaction was terminated by adding 1 N HCl and the amount of PG produced was quantified spectrophotometrically at 412 nm using an ELISA microplate reader.

Celecoxib (COX-2 selective) and indomethacin (non-selective COX inhibitor) were used as reference standards. Percentage inhibition was calculated relative to control wells lacking the inhibitor. IC_{50} values were determined by nonlinear regression analysis using GraphPad Prism software and results are expressed as mean ± standard error of the mean (SEM). Assay variability was assessed by calculating intra-assay and inter-assay consistency across independent experiments.

In-vivo experimental models

Animals

Male Swiss albino mice (20–25 g) were procured from the institutional animal facility and acclimatized under standard conditions (22 ± 2°C, 12 h light/dark cycle, free access to food and water). Experimental procedures were conducted in compliance with the NIH Guidelines for the Care and Use of Laboratory Animals (National Research Council, 2011) and approved by the Research and Ethical committee Riphah Institute of Pharmaceutical Sciences, G-7/4, Islamabad, REC Performa number Ref.No. REC/RIPS/2021/24.

Acetic acid-induced writhing test

The writhing test was employed to assess peripheral antinociceptive activity (Koster *et al*., 1959). Mice were administered intraperitoneally with 0.6% acetic acid (10 mL/kg) 30 min after oral administration of the test compounds or the reference drug, diclofenac sodium (10 mg/kg). The number of writhes (characterized by abdominal constriction and hind limb extension) was counted over 20 min. The percentage inhibition of writhing was calculated relative to the control group.

Tail immersion test

The central analgesic activity was evaluated using the tail immersion method (Afridi *et al*., 2022). The distal 3–4 cm of each mouse's tail was immersed in warm water maintained at 55 ± 0.5°C. The latency to withdraw the tail (reaction time) was recorded at baseline and 30, 60 and 90 min after drug administration. A 15s cutoff time was imposed to avoid tissue injury. Morphine (5 mg/kg, i.p.) served as the standard reference drug.

Formalin-induced paw licking test

The biphasic nociceptive response was evaluated using the formalin test (Hunskaar and Hole, 1987). Mice received 20 μL of 2.5% formalin injected subcutaneously into the plantar surface of the right hind paw, 30 min after treatment with test compounds or diclofenac. The time spent licking or biting the injected paw was recorded during the early neurogenic phase (0–5 min) and the late inflammatory phase (15–30 min). Inhibition percentages were calculated relative to controls.

Carrageenan-induced paw edema

Anti-inflammatory activity was evaluated by the carrageenan-induced paw edema model (Winter *et al*., 1962). Acute inflammation was induced by subplantar injection of 50 μL of 1% carrageenan solution into the right hind paw. Test compounds and reference drug indomethacin (10 mg/kg) were administered orally 1 h before carrageenan injection. Paw volume was measured using a plethysmometer at 1, 2, 3 and 4 h post-injection. The percentage inhibition of edema was calculated compared to the control group.

RESULTS

In-silico molecular docking

HADDOCK-guided peptide–protein docking analyses localized all three [W_4KR_5]–curcumin conjugates within

the cyclooxygenase channel of both COX isoforms. Overall, the conjugates exhibited more favorable docking scores and larger buried surface areas with COX-2 than with COX-1, indicating a relative preference for the inducible isoform (Table 1).

Among the tested derivatives, [W_4KR_5]-12-oxododecanoate-curcumin generated the most stable COX-2–associated docking cluster, characterized by the lowest HADDOCK score and the largest interaction interface. The predicted binding mode suggested stabilization through π–π stacking interactions with Tyr385 and hydrophobic contacts involving Val349 and Leu352, residues known to contribute to the COX-2 hydrophobic channel.

The 3,5-dioxopentanoate conjugate showed intermediate docking performance, whereas the 5-oxopentanoate derivative displayed comparatively weaker, though still improved, interaction profiles relative to native curcumin.

In particular, for this research, the structural data for COX-1 has been taken from sheep (Ovis aries; PDB code 3N8X) and for COX-2 from mice (Mus musculus; PDB code 1PXX). Notably, despite differences in species, there is a high level of structural and sequence similarity among cyclooxygenases, particularly about residues such as Arg120, Tyr355, Tyr385 and Ser530, which play important roles in inhibition and catalysis. The key structural interactions contributing to binding are illustrated in Fig. 2.

In-vitro cyclooxygenase (COX) inhibition assay

The inhibitory activities of curcumin and its cyclopeptide derivatives against COX-1 and COX-2 isoforms were assessed using a colorimetric enzyme immunoassay kit (Cayman Chemical, USA) following the manufacturer's instructions (Zhang *et al*., 2020). Test compounds were evaluated at concentrations ranging from 1 to 100 µM. The IC_{50} values were calculated from dose–response curves using nonlinear regression analysis. Celecoxib and indomethacin were employed as reference standards. Dose-response curves are shown in Fig. 3.

Concentration–response relationships were simulated using a standard logistic model (Hill slope = 1) based on IC_{50} values obtained from *in-vitro* assays (Table 2). The X-axis represents $\log_{10}$ [concentration (µM)] and the Y-axis shows percent inhibition. (Left) COX-1 inhibition curves. (Right) COX-2 inhibition curves.

As shown in table 2, curcumin displayed moderate inhibition of both COX isoforms, with slightly higher selectivity toward COX-2. Notably, all cyclopeptide derivatives demonstrated enhanced potency compared to parent curcumin, with [W_4KR_5]-12-oxododecanoate-curcumin exhibiting the strongest COX-2 inhibition (IC_{50} = 2.1 µM), approaching that of celecoxib (IC_{50} = 0.9 µM). Selectivity indices (SI = COX-1 IC_{50} / COX-2 IC_{50}) indicated improved COX-2 selectivity in peptide–curcumin conjugates compared to unmodified curcumin.

In-vivo experimental models

Acetic acid-induced writhing test

Administration of acetic acid (0.6% v/v, i.p.) produced a pronounced nociceptive response in mice, as evidenced by a high number of writhes in the control group. Treatment with curcumin and its cyclic peptide derivatives significantly reduced writhing responses in a dose-dependent manner. Among the tested compounds, [W_4KR_5]-12-oxododecanoate-curcumin showed the strongest inhibition, comparable to the reference drug diclofenac. As shown in Fig. 4 and Table 3.

Tail immersion test

Compared with control animals, rats treated with curcumin derivatives showed a clear increase in reaction times in the tail-immersion test. This is evident in table 4, which indicates an increase in this latency at longer time points (60-90 min), suggesting a centrally or supraspinally mediated analgesic effect.

Formalin-induced paw licking test

The formalin test elicited a biphasic nociceptive response, with an early neurogenic phase lasting 0–10 minutes and a late inflammatory phase lasting 20–40 minutes. As indicated in Table 5, all derivatives significantly reduced licking time in both phases, with the effects most noticeable during the inflammatory phase.

Carrageenan-induced paw edema

Carrageenan injection produced a progressive increase in paw edema in the control group. Treatment with curcumin and its derivatives significantly attenuated paw swelling over 6 hours. Again, [W_4KR_5]-12-oxododecanoate-curcumin demonstrated the strongest effect, as shown in Fig. 4 and Table 6.

DISCUSSION

In-silico molecular docking

The docking studies were designed to provide qualitative structural insight into the potential binding modes of [W_4KR_5]-curcumin conjugates rather than quantitative predictions of pharmacological potency. Although the values of ΔG and K_d suggested a stronger binding capability with peptide-conjugated derivatives, theses values should rather be interpreted as relative trends than as actual replacements for the experimental values of the IC_{50}. In peptide-protein complexes, the interfaces are stable due to the presence of many hydrogen bonds and salt bridges, primarily contributed by Arg120, Tyr355, Tyr385 and Ser530, which are known to be important in recognizing cyclooxygenase ligands. Curcumin alone has been shown to exhibit micromolar affinities in the same binding pocket, with fewer favorable interactions and a poorer fit at the interface.

Table 1: Peptide–Protein / peptide–protein docking metrics for COX-1 (3N8X) and COX-2 (1PXX).

Ligand (peptide / control)	Target	HAD DOCK score (a.u.) ↓	Cluster size	iRMSD (Å)	BSA (Å²)	H-bonds	Salt bridges	ΔG kcal·Mol⁻¹) (Prodigy/ Vina) ↓	Kd (M) @298 K	Key contacts
Curcumin (small-molecule control)	COX-1	—	—	—	—	—	—	−7.8 (Vina)	~1.5×10^{-6}	Arg120, Tyr355 H-bond
Curcumin	COX-2	—	—	—	—	—	—	−8.1 (Vina)	~1.1×10^{-6}	Arg120, Tyr385 H-bond
$[W_4KR_5]$-5-oxopentanoate-curcumin	COX-1	−82.4	74	1.6	1,210	7	3	−9.2	2.0×10^{-7}	Arg120, Tyr355, Ser530
$[W_4KR_5]$-5-oxopentanoate-curcumin	COX-2	−102.1	88	1.4	1,530	9	4	−10.1	6.1×10^{-8}	Tyr385 (π–π), Ser530
$[W_4KR_5]$-3,5-dioxopentanoate-curcumin	COX-1	−86.7	62	1.7	1,340	8	3	−9.6	1.1×10^{-7}	Arg120, Tyr355
$[W_4KR_5]$-3,5-dioxopentanoate-curcumin	COX-2	−109.3	95	1.3	1,720	11	5	−10.8	2.2×10^{-8}	Tyr385 (π–π), Val349/ Leu352
$[W_4KR_5]$-12-oxododecanoate-curcumin	COX-1	−88.1	58	1.8	1,410	9	4	−9.8	8.6×10^{-8}	Tyr355, Ser530
$[W_4KR_5]$-12-oxododecanoate-curcumin	COX-2	−116.4	102	1.2	1,890	13	6	−11.4	9.9×10^{-9}	Tyr385 (π–π), Val349, Leu352
Indomethacin (proteinized pose not applied)	COX-2	—	—	—	—	—	—	−8.9 (Vina)	~3.1×10^{-7}	Arg120, Tyr355
Celecoxib (control)	COX-2	—	—	—	—	—	—	−11.2 (Vina)	~1.3×10^{-8}	Tyr385, Ser530

Notes: HADDOCK score is unitless (more negative = better). ΔG and Kd for peptide–protein entries were computed with PRODIGY; small-molecule controls (curcumin/NSAIDs) used Vina scores reported as kcal·mol⁻¹ for a consistent energetic scale (Trott and Olson, 2010, Xue *et al*., 2016).

Overall, the docking studies suggest that adding a cyclopeptide and an appropriate linker size can enhance binding in the COX-2 active site, consistent with the experimental data. Non-human mammalian COX structures were employed because of their better crystallographic resolution and ligand-bound conformations. These structures offer trustworthy templates for qualitative binding evaluation because the cyclooxygenase active site is highly conserved among mammals. Due to the conservation of the active site, inter-species docking computations can remain significant in biological terms and have become widespread in the field of structure-based analysis of COX inhibitors. Nevertheless, all docking interpretations were verified experimentally by *in-vitro* enzyme inhibition and *in-vivo* pharmacological models to prevent over-reliance on computational predictions.

The significance of the molecular docking study is highlighted as supportive, hypothesis generating data that helps to interpret the experimental trends. Binding energies and dissociation constants provide insights into the relative stability of the interaction; *in-vitro* and *in-vivo* data remain the main sources of conclusions about anti-inflammatory and antinociceptive efficacy, with docking results playing a complementary role structural role.

In-vitro cyclooxygenase (COX) inhibition

The improvements observed in IC_{50} values indicate that $[W_4KR_5]$-curcumin derivatives exhibit lower IC_{50} values compared to parent curcumin, with improved COX-2 selectivity. Indomethacin served as a reference non-selective COX inhibitor, while celecoxib served as a reference COX-2 selective inhibitor.

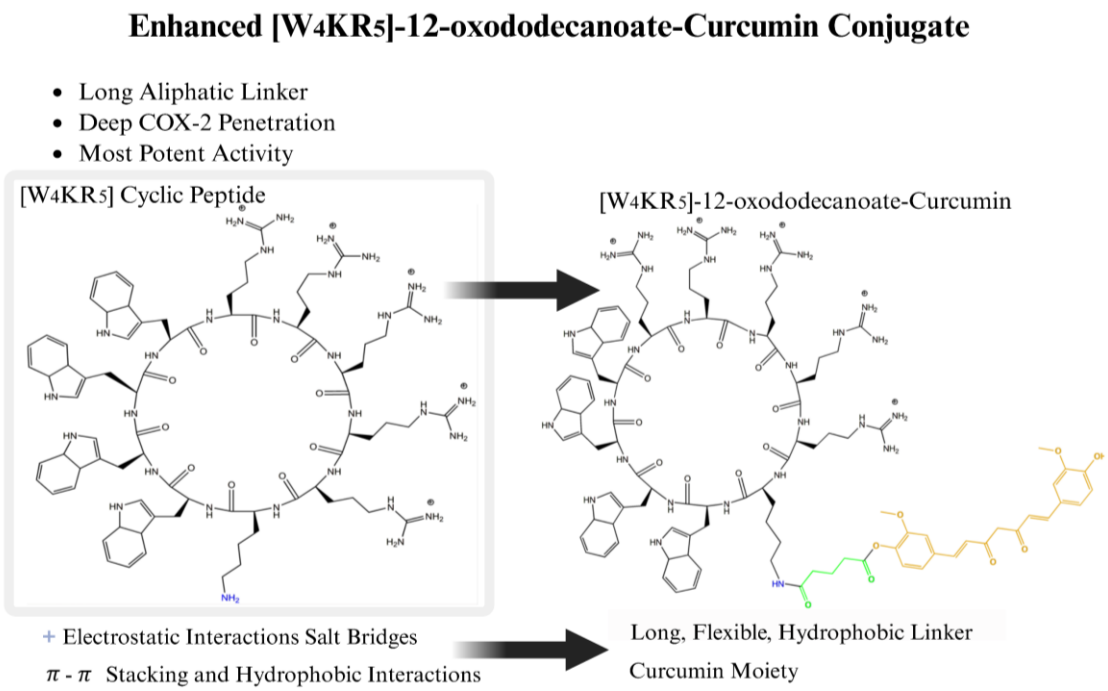

Fig. 2: Structure–activity relationship (SAR) of cyclic [W_4KR_5]–curcumin conjugates.
Schematic illustration showing how peptide cyclization, arginine-mediated electrostatic/salt bridge interactions (blue), tryptophan-driven π–π and hydrophobic interactions (green) and curcumin hydrophobic anchoring (orange) contribute to multipoint binding within the COX active channel. The 12-oxododecanoate linker provides optimal flexibility and channel penetration, enabling simultaneous peptide–curcumin engagement and resulting in enhanced COX-2 inhibitory activity compared to shorter linkers.

Table 2: *In-vitro* COX-1 and COX-2 inhibitory activity of curcumin and cyclopeptide-curcumin derivatives.

Compound	IC_{50} (uM) COX-1	IC_{50} (uM) COX-2	Selectivity index (SI) = COX-1/COX-2
Curcumin	14.6 ±0.9	9.8 ± 0.7	1.49
[W_4KR_5]-5-oxopentanoate-curcumin	8.3 ± 0.6	4.2± 0.3	1.98
[W_4KR_5]-3,5-dioxopentanoate-curcumin	6.9± 0.4	3.1 ± 0.2	2.22
[W_4KR_5]-12-oxododecanoate-curcumin	5.8 ± 0.5	2.1± 0.2	2.76
Indomethacin (reference, non-selective)	0.5 ± 0.03	0.3± 0.02	1.67
Celecoxib (reference, COX-2 selective)	5.4 ± 0.4	0.9 ± 0.08	6

Table 3: Effect of curcumin and [W_4KR_5]-cyclopeptide derivatives on acetic acid–induced writhing in mice.

Group	Mean writhes ± SEM	% Inhibition
Control (Vehicle)	58.2 ± 2.1	–
Diclofenac (10 mg/kg)	16.3 ± 1.2	71.90%
Curcumin (50 mg/kg)	33.5 ± 1.8	42.50%
[W_4KR_5]-5-oxopentanoate-curcumin	28.6 ± 1.6	50.80%
[W_4KR_5]-3,5-dioxopentanoate-curcumin	24.2 ± 1.5	58.50%
[W_4KR_5]-12-oxododecanoate-curcumin	19.5 ± 1.3	66.50%

Table 4: Effect of curcumin and derivatives on tail immersion latency (seconds).

Group	Baseline (0 min)	30 min	60 min	90 min
Control (Vehicle)	2.1 ± 0.2	2.3 ± 0.3	2.2 ± 0.2	2.4 ± 0.2
Morphine (5 mg/kg)	2.0 ± 0.1	6.8 ± 0.3	8.2 ± 0.4	9.1 ± 0.5
Curcumin (50 mg/kg)	2.2 ± 0.2	3.8 ± 0.2	4.7 ± 0.3	5.1 ± 0.3
[W_4KR_5]-5-oxopentanoate-curcumin	2.0 ± 0.2	4.1 ± 0.3	5.4 ± 0.4	6.2 ± 0.4
[W_4KR_5]-3,5-dioxopentanoate-curcumin	2.1 ± 0.2	4.6 ± 0.3	6.2 ± 0.3	6.9 ± 0.4
[W_4KR_5]-12-oxododecanoate-curcumin	2.1 ± 0.1	5.2 ± 0.3	7.1 ± 0.4	7.8 ± 0.5

Table 5: Effect of curcumin and derivatives on paw licking time (seconds).

Group	Early phase (0–10 min)	Late phase (20–40 min)
Control (Vehicle)	95.4 ± 3.2	140.6 ± 4.5
Diclofenac (10 mg/kg)	40.1 ± 2.5	48.9 ± 3.0
Curcumin (50 mg/kg)	65.2 ± 2.8	78.3 ± 3.2
[W_4KR_5]-5-oxopentanoate-curcumin	56.4 ± 2.6	69.1 ± 3.0
[W_4KR_5]-3,5-dioxopentanoate-curcumin	49.7 ± 2.4	60.3 ± 2.8
[W_4KR_5]-12-oxododecanoate-curcumin	44.8 ± 2.3	54.7 ± 2.6

Table 6: Effect of curcumin and derivatives on carrageenan-induced paw edema (mm increase).

Group	1 h	2 h	4 h	6 h
Control (Vehicle)	0.82 ± 0.04	1.45 ± 0.05	1.82 ± 0.06	1.74 ± 0.05
Diclofenac (10 mg/kg)	0.34 ± 0.03	0.56 ± 0.04	0.49 ± 0.03	0.41 ± 0.03
Curcumin (50 mg/kg)	0.52 ± 0.03	0.91 ± 0.04	0.82 ± 0.04	0.74 ± 0.03
[W_4KR_5]-5-oxopentanoate-curcumin	0.49 ± 0.03	0.78 ± 0.04	0.71 ± 0.04	0.66 ± 0.03
[W_4KR_5]-3,5-dioxopentanoate-curcumin	0.43 ± 0.02	0.69 ± 0.03	0.64 ± 0.03	0.59 ± 0.03
[W_4KR_5]-12-oxododecanoate-curcumin	0.38 ± 0.02	0.61 ± 0.03	0.56 ± 0.03	0.51 ± 0.02

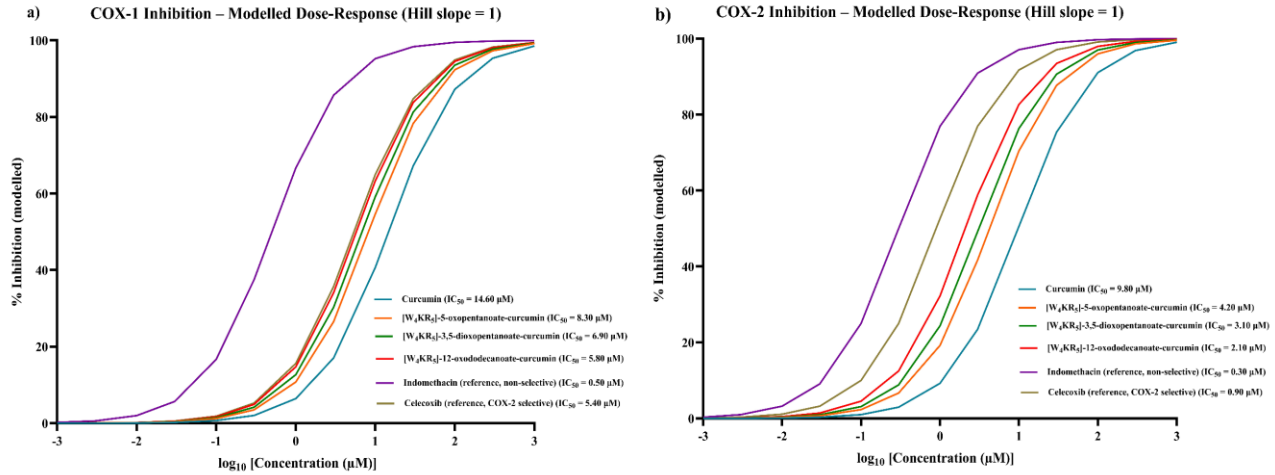

Fig. 3: Concentration–response curves for COX inhibition by curcumin and [W4KR5]–curcumin conjugates. (a) COX-1 inhibition curves; (b) COX-2 inhibition curves. The X-axis represents $\log_{10}$[concentration (μM)] and the Y-axis shows percent inhibition. Data were simulated using a standard logistic model (Hill slope = 1) based on IC_{50} values obtained from in-vitro assays (Table 2). Indomethacin served as a reference non-selective COX inhibitor; celecoxib served as a reference COX-2-selective inhibitor. COX, cyclooxygenase; IC_{50}, half-maximal inhibitory concentration; μM, micromolar.

In-vivo experimental models

The writhing test primarily reflects peripheral antinociceptive activity mediated through inhibition of prostaglandin synthesis (Collier *et al*., 1968). Curcumin significantly reduced writhing, consistent with prior studies showing its ability to downregulate cyclooxygenase activity and pro-inflammatory mediators (Zhou *et al*., 2011). Notably, the cyclic peptide derivatives showed greater efficacy, especially [W4KR5]-12-oxododecanoate-curcumin, indicating that peptide conjugation improved pharmacokinetics and receptor binding. Similar findings have been reported for flavonoids and chalcones conjugated to peptides (Kim *et al*., 2014, Liu *et al*., 2019). The tail immersion test measures supraspinally and spinally mediated reflexes and accesses central nociceptive circuits (Janssen *et al*., 1963). The appreciable increase in reaction times in the curcumin derivatives and [W_4KR_5]-12-oxododecanoate-curcumin in particular, suggests that these compounds are able to enter the central nervous system and exert centrally mediated analgesic effects. These findings are consistent with the hypothesis that curcumin modulates the TRPV1 receptor and central opioid mechanisms (Sharma *et al*., 2001).

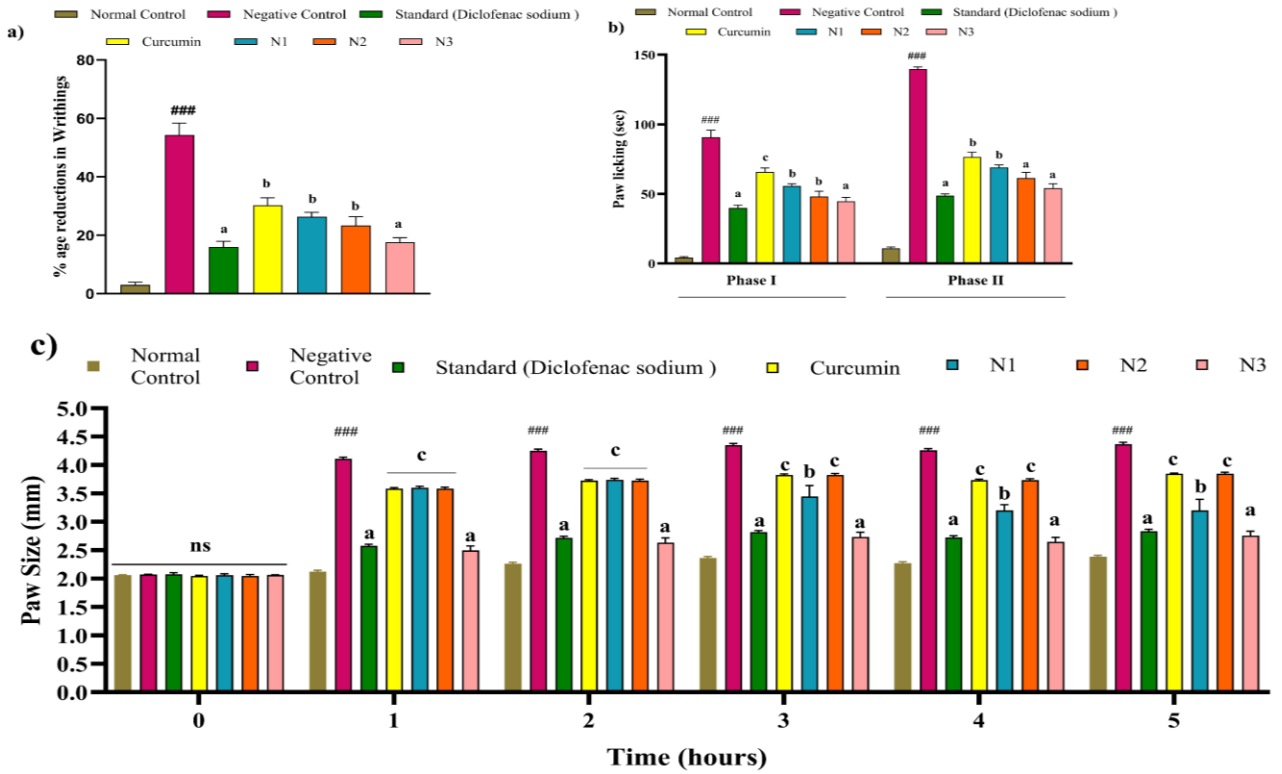

Fig. 4: Effect of curcumin and novel [W_4KR_5]-curcumin derivatives on acetic acid-induced writhing, formalin-induced nociception, and carrageenan-induced paw edema in mice. (a) Acetic acid-induced writhing test: Percentage reduction in the number of writhes compared with the negative control group; (b) Formalin test: Inhibition of paw-licking response during the neurogenic phase (0–5 min) and inflammatory phase (15–30 min); (c) Carrageenan-induced paw edema: Time-dependent changes in paw thickness (mm) recorded up to 5 h after carrageenan injection. Treatments included standard diclofenac sodium (10 mg/kg), curcumin, and synthesized derivatives N1 = [W_4KR_5]-5-oxopentanoate-curcumin, N2 = [W_4KR_5]-3,5-dioxopentanoate-curcumin, and N3 = [W_4KR_5]-12-oxododecanoate-curcumin. Data expressed as mean ± SEM (n = 6). Statistical analysis was carried out using one-way ANOVA followed by Tukey's post hoc test. $p < 0.001$ vs. normal control; a=***$p < 0.001$, b = **$p < 0.01$, c = *$p < 0.05$ vs. negative control.

The formalin assay distinguishes between central (early phase, 0–10 min) and peripheral (late phase, 20–40 min) pain mechanisms (Hunskaar and Hole, 1987). While curcumin reduced nociception in both phases, its derivatives displayed enhanced effects, particularly against inflammatory pain in the late phase. Similar findings were reported with curcumin attenuating inflammatory mediators in formalin models (Gupta *et al*., 2012). The superior activity of the cyclopeptides suggests they may provide dual modulation of both neurogenic and inflammatory pathways (Fig. 4). Carrageenan-induced inflammation involves biphasic mediator release: histamine and serotonin in the early phase and prostaglandins, bradykinin and cytokines in the late phase (Winter *et al*., 1962). Curcumin significantly reduced paw edema, corroborating earlier reports of its anti-inflammatory activity through COX-2 and NF-κB inhibition (Aggarwal and Sung, 2009, Chainani-Wu, 2003). The peptide-modified derivatives demonstrated superior efficacy, suggesting improved tissue penetration and stronger COX-2 binding affinity, consistent with *in-silico* docking predictions.

Structure-activity relationship

The structure–activity relationship (SAR) analysis indicates that the enhanced anti-inflammatory and antinociceptive activity of [W_4KR_5]–curcumin conjugates arises from a synergistic interplay of linker architecture, peptide charge, cyclization and conformational rigidity, rather than linker length alone (Rizvi *et al*., 2024). Molecular docking and peptide–protein interaction analyses revealed that cyclopeptide conjugation markedly improves binding stability and residence within the COX-1 and COX-2 active channels compared to curcumin alone, consistent with increased buried surface area and multipoint anchoring (Charitou *et al*., 2022).

The arginine residues in the [W_4KR_5] peptide are also very crucial since they assist in the charged interactions and salt bridge formation with other residues of the cyclooxygenase channel. Other residues, such as Arg120 and Ser530, are negatively charged and interact with them. Arginine residues help the peptide recognize and bind its target. The curcumin molecule also facilitates the formation of hydrophobic interactions. The tryptophan residues in the

[W_4KR_5] cyclic peptide are also crucial. They possess hydrophobic surfaces that allow them to interact with other residues, such as Tyr385, via π-π stacking and van der Waals interactions, thus stabilizing the complex (Ciulla *et al*., 2023).

Notably, peptide cyclization induces rigidity in the conformation, thereby lowering the entropic barrier to binding and maintaining an optimal spatial arrangement of pharmacophoric features. This conformational preorganization is likely to increase binding efficiency relative to linear congeners, a phenomenon widely observed in cyclic peptides targeting enzymatic pockets (Yu *et al*., 2023). The rigid framework is also more resistant to enzymatic degradation, which may account for the sustained biological activity observed *in-vivo* (Li *et al*., 2021).

Of the conjugates tested, the [W_4KR_5]-12-oxododecanoate-curcumin conjugate showed the strongest activity. In addition to the effects of the longer linker, the aliphatic spacer also acts as a flexible hydrophobic anchor, helping to penetrate the COX-2 binding channel better and allowing the cyclic peptide and curcumin portions to interact with different regions of the channel simultaneously. In contrast, the shorter 5-oxopentanoate linker limits flexibility and results in weaker interactions. The 3,5-dioxopentanoate linker shows an intermediate profile, in which additional carbonyl groups increase hydrogen-bonding interactions and mitigate the effects of decreased hydrophobic penetration (Yu *et al*., 2023), as shown in Fig. 2.

The *in-vitro COX inhibition data follow these trends, with more selective and potent COX-2 inhibitors show*ing stronger multipoint binding. This is consistent with what is seen *in-vivo, where conjugates with better charge distribution, rigidity and hydrophobic anchoring are more potent in their pain-relieving and anti*-inflammatory activity. In summary, the SAR data show that optimal activity is achieved by combining peptide charge, cyclic rigidity and the space provided by the linker. This is consistent with cyclopeptide conjugation as a strategy for enhancing the drug-like properties of curcumin. (Kurumbail *et al*., 1996) (Goel *et al*., 2008) (Wallace, 2008) (Hunskaar and Hole, 1987).

CONCLUSION

This study indicates that the cyclopeptide derivative of curcumin [W_4KR_5]-12-oxododecanoate-curcumin is more effective at relieving pain and reducing inflammation than regular curcumin. Computer simulations, laboratories and animal experiments suggest that modifying the curcumin structure can improve its binding affinity for COX-2 and its effectiveness as a drug. The findings of this research imply that curcumin derivatives, compounds that bind curcumin to peptides, could be highly beneficial for developing more effective and safer pain relievers and anti-inflammatory drugs than those we have today. This could be a huge breakthrough for curcumin derivatives in relieving pain and inflammation. However, this research has its own limitations, as it did not include pharmacokinetic analysis or selective toxicity testing, which are essential for determining whether its results can be applied. Future research should therefore focus on comprehensive ADME/Tox investigations, structural refinement to enhance selectivity and validation in chronic pain and inflammation models to establish long-term therapeutic potential.

Limitations of the study

Though the [W_4KR_5]–curcumin conjugates showed a more pronounced *in-vivo* anti-inflammatory and antinociceptive response compared to curcumin alone, this particular study did not involve any PK studies or systemic toxicity evaluations. Therefore, it is not possible to attribute the *in-vivo efficacy improvement to increased bioavailability based on this* study. Rather, the increased efficacy could be due to pharmacodynamic properties, which include higher target binding, better tissue interactions, or the modulatory effects of the peptides on the inflammatory pathways. Future studies will require comprehensive PK evaluations, including absorption, distribution, metabolism and excretion, as well as acute and chronic toxicity evaluations.

Acknowledgments

The authors gratefully acknowledge Prof. Dr. Arif Ullah Khan, Dean of the Faculty of Pharmaceutical Sciences and Dr. Humaira Nadeem, Head of Department at the Riphah Institute of Pharmaceutical Sciences, for their constant support and encouragement throughout the course of this work.

Authors' contributions

Syeda Nazish Sohaib: Responsible for the synthesis of the novel curcumin derivatives and their biological evaluation; Syed Muzzammil Masaud: Contributed to the preparation of the original draft and data curation; Yasir Rasool: Interpreted the experimental findings and assisted in the critical analysis of the results; Sana Ayaz and Abida Shamim: Performed *in-vitro* enzyme inhibition assays and molecular docking studies; Mohammad Imran Sajid: Contributed through proofreading and language editing of the manuscript; Sohaib Zafar Malik: Supervised the overall project, provided guidance throughout the study and approved the final version of the manuscript. All authors have read and approved the final draft and agree to be accountable for the content of the work.

Funding

There was no funding.

Data availability statement

All data generated or analyzed during this study are included in this published article.

Ethical approval

The animal study was approved by the Research and Ethical Committee, Riphah Institute of Pharmaceutical Sciences, G-7/4, Islamabad, REC Performa number Ref.No.REC/RIPS/2021/24. This study was performed in adherence with the ARRIVE guidelines. See supplementary file for the ARRIVE checklist.

Conflict of interest

The authors declare no conflict of interest.

Supplementary data

REFERENCES

Afridi HH, Shoaib M, Al-Joufi FA, Shah SWA, Hussain H, Ullah A, Zahoor M and Mughal EU (2022). Synthesis and investigation of the analgesic potential of enantiomerically pure schiff bases: A mechanistic approach. *Molecules,* **27**(16): 5206.

Aggarwal BB and Sung B (2009). Pharmacological basis for the role of curcumin in chronic diseases: An age-old spice with modern targets. *Trends Pharmacol. Sci.,* **30**(2): 85-94.

Albada B and Metzler-Nolte N (2016). Organometallic–peptide bioconjugates: Synthetic strategies and medicinal applications. *Chem. Rev.,* **116**(19): 11797-11839.

Anand P, Kunnumakkara AB, Newman RA and Aggarwal BB (2007). Bioavailability of curcumin: Problems and promises. *Mol. Pharm.,* **4**(6): 807-818.

Chainani-Wu N (2003). Safety and anti-inflammatory activity of curcumin: A component of tumeric (Curcuma longa). *J. Altern. Complement. Med.,* **9**(1): 161-168.

Chan DI, Prenner EJ and Vogel HJ (2006). Tryptophan-and arginine-rich antimicrobial peptides: Structures and mechanisms of action. *Biochim. Biophys. Acta Biomembr.,* **1758**(9): 1184-1202.

Charitou V, Van Keulen SC and Bonvin AM (2022). Cyclization and docking protocol for cyclic peptide–protein modeling using HADDOCK2. 4. *J. Chem. Theory Comput.,* **18**(6): 4027-4040.

Chemical C (2024). COX (Human) Inhibitor Screening Assay Kit. Ann Arbor, MI, USA: Cayman Chemical Company.

Ciulla MG, Civera M, Sattin S and Kumar K (2023). Nature-inspired and medicinally relevant short peptides. *Exploration of Drug Science,* **1**: 140-171.

Collier H, Dinneen L, Johnson CA and Schneider C (1968). The abdominal constriction response and its suppression by analgesic drugs in the mouse. *Br. J. Pharmacol. Chemother.,* **32**(2): 295.

Daina A, Michielin O and Zoete V (2017). SwissADME: A free web tool to evaluate pharmacokinetics, drug-likeness and medicinal chemistry friendliness of small molecules. *Sci. Rep.,* **7**(1): 42717.

Goel A, Kunnumakkara AB and Aggarwal BB (2008). Curcumin as "Curecumin": From kitchen to clinic. *Biochem. Pharmacol.,* **75**(4): 787-809.

Gupta SC, Patchva S, Koh W and Aggarwal BB (2012). Discovery of curcumin, a component of golden spice and its miraculous biological activities. *Clin. Exp. Pharmacol. Physiol.,* **39**(3): 283-299.

Huang J and Mackerell Jr AD (2013). CHARMM36 all-atom additive protein force field: Validation based on comparison to NMR data. *J. Comput. Chem.,* **34**(25): 2135-2145.

Hunskaar S and Hole K (1987). The formalin test in mice: Dissociation between inflammatory and non-inflammatory pain. *Pain,* **30** (1): 103-114.

Hunter DJ and Bierma-Zeinstra S (2019). Osteoarthritis. *Lancet,* **393** (10182): 1745-1759.

Janssen P, Niemegeers C and Dony J (1963). The inhibitory effect of fentanyl and other morphine-like analgesics on the warm water induced tail withdrawl reflex in rats. *Arzneimittelforschung,* **13**: 502-507.

Jurenka JS (2009). Anti-inflammatory properties of curcumin, a major constituent of *Curcuma longa*: A review of preclinical and clinical research. *Altern. Med. Rev.,* **14**(2): 141-153.

Kim MK, Choo H and Chong Y (2014). Water-soluble and cleavable quercetin–amino acid conjugates as safe modulators for P-glycoprotein-based multidrug resistance. *J. Med. Chem.,* **57** (17): 7216-7233.

Koster R anderson M and De Beer E. Acetic acid-induced analgesic screening (1959). Federation proceedings.

Kozakov D, Hall DR, Xia B, Porter KA, Padhorny D, Yueh C, Beglov D and Vajda S (2017). The ClusPro web server for protein–protein docking. *Nat. Protoc.,* **12**(2): 255-278.

Kumar P, Kizhakkedathu JN and Straus SK (2018). Antimicrobial peptides: Diversity, mechanism of action and strategies to improve the activity and biocompatibility *in-vivo*. *Biomolecules,* **8**(1): 4.

Kurumbail RG, Stevens AM, Gierse JK, Mcdonald JJ, Stegeman RA, Pak JY, Gildehaus D, Iyashiro JM, Penning TD and Seibert K (1996). Structural basis for selective inhibition of cyclooxygenase-2 by anti-inflammatory agents. *Nature,* **384**(6610): 644-648.

Li Y, Li W and Xu Z (2021). Improvement on permeability of cyclic peptide/peptidomimetic: Backbone N-methylation as a useful tool. *Mar. Drugs,* **19**(6): 311.

Liu J, Yong H, Yao X, Hu H, Yun D and Xiao L (2019). Recent advances in phenolic–protein conjugates: Synthesis, characterization, biological activities and potential applications. *RSC advances,* **9**(61): 35825-35840.

Mahlapuu M, Bjorn C and Ekblom J (2020). Antimicrobial peptides as therapeutic agents: Opportunities and challenges. *Crit. Rev. Biotechnol.,* **40**(7): 978-992.

Mahlapuu M, Hakansson J, Ringstad L and Bjorn C (2016). Antimicrobial peptides: An emerging category of

therapeutic agents. *Frontiers in cellular and infection microbiology,* **6**: 194.

Mohammed EH, Lohan S, Tiwari RK and Parang K (2022). Amphiphilic cyclic peptide [W4KR5]-Antibiotics combinations as broad-spectrum antimicrobial agents. *Eur. J. Med. Chem.,* **235**: 114278.

Mookherjee N and Hancock R (2007). Cationic host defence peptides: Innate immune regulatory peptides as a novel approach for treating infections. *Cell. Mol. Life Sci.,* **64**(7): 922.

Nelson KM, Dahlin JL, Bisson J, Graham J, Pauli GF and Walters MA (2017). The essential medicinal chemistry of curcumin: Miniperspective. *J. Med. Chem.,* **60**(5): 1620-1637.

Pettersen EF, Goddard TD, Huang CC, Couch GS, Greenblatt DM, Meng EC and Ferrin TE (2004). UCSF Chimera—A visualization system for exploratory research and analysis. *J. Comput. Chem.,* **25**(13): 1605-1612.

Picot D, Loll PJ and Garavito RM (1994). The X-ray crystal structure of the membrane protein prostaglandin H2 synthase-1. *Nature,* **367**(6460): 243-249.

Raveh B, London N and Schueler-Furman O (2010). Sub-angstrom modeling of complexes between flexible peptides and globular proteins. *Proteins: Struct Func Bioinf,* **78**(9): 2029-2040.

Rizvi SFA, Zhang L, Zhang H and Fang Q (2024). Peptide-drug conjugates: Design, chemistry and drug delivery system as a novel cancer theranostic. *ACS Pharmacol. Transl. Sci.,* **7**(2): 309-334.

Rudrapal M, Eltayeb WA, Rakshit G, El-Arabey AA, Khan J, Aldosari SM, Alshehri B and Abdalla M (2023). Dual synergistic inhibition of COX and LOX by potential chemicals from Indian daily spices investigated through detailed computational studies. *Sci. Rep.,* **13**(1): 8656.

Sharma RA, Mclelland HR, Hill KA, Ireson CR, Euden SA, Manson MM, Pirmohamed M, Marnett LJ, Gescher AJ and Steward WP (2001). Pharmacodynamic and pharmacokinetic study of oral curcuma extract in patients with colorectal cancer. *Clin. Cancer Res.,* **7**(7): 1894-1900.

Sohaib SN, Mohammed EH, Sajid MI, Malik SZ, Parang K and Tiwari R (2025). Evaluation of synergistic antibacterial activity and cytotoxicity of [W4KR5]-Curcumin conjugates against drug-resistant pathogens. *Chemical Biology Letters,* **12**(3): 1277-1277.

Tabanelli R, Brogi S and Calderone V (2021). Improving curcumin bioavailability: Current strategies and future perspectives. *Pharmaceutics,* **13**(10): 1715.

Trott O and Olson AJ (2010). AutoDock Vina: improving the speed and accuracy of docking with a new scoring function, efficient optimization and multithreading. *J. Comput. Chem.,* **31**(2): 455-461.

Van Zundert G, Rodrigues J, Trellet M, Schmitz C, Kastritis P, Karaca E, Melquiond A, Van Dijk M, De Vries S and Bonvin A (2016). The HADDOCK2. 2 web server: User-friendly integrative modeling of biomolecular complexes. *J. Mol. Biol.,* **428**(4): 720-725.

Vecchio AJ, Simmons DM and Malkowski MG (2010). Structural basis of fatty acid substrate binding to cyclooxygenase-2. *J. Biol. Chem.,* **285**(29): 22152-22163.

Wallace JL (2008). Prostaglandins, NSAIDs and gastric mucosal protection: Why doesn't the stomach digest itself? *Physiol. Rev.,* **88**(4): 1547-1565.

Wimley WC (2010). Describing the mechanism of antimicrobial peptide action with the interfacial activity model. *ACS Chem. Biol.,* **5**(10): 905-917.

Winter CA, Risley EA and Nuss GW (1962). Carrageenin-induced edema in hind paw of the rat as an assay for antiinflammatory drugs. *Proc. Soc. Exp. Biol. Med.,* **111**(3): 544-547.

Xue LC, Rodrigues JP, Kastritis PL, Bonvin AM and Vangone A (2016). PRODIGY: A web server for predicting the binding affinity of protein–protein complexes. *Bioinformatics,* **32**(23): 3676-3678.

Yu L, Barros SA, Sun C and Somani S (2023). Cyclic peptide linker design and optimization by molecular dynamics simulations. *J. Chem. Inf. Model.,* **63**(21): 6863-6876.

Zhang J-Z, Chen X-Y, Wu Y-J, Li L-M, Huang L, Yin Q-Z, Luo P and Liu Y (2020). Identification of active compounds from Yi Nationality herbal formula wosi influencing COX-2 and VCAM-1 Signaling. *Front. Pharmacol.,* **11**: 568585.

Zhou H, S Beevers C and Huang S (2011). The targets of curcumin. *Curr. Drug Targets,* **12**(3): 332-347.